

3  
4 **Running title:** BATF2 reverse MDR in GC

5  
6 **BATF2 reverses multidrug resistance of gastric cancer cells and centrosome clustering by**  
7 **suppressing ATM phosphorylation**

8  
9 Wei Yang<sup>1</sup>, Jianlin Song<sup>1</sup>, Lixia Jiang<sup>1</sup>, Wenchuan Zhu<sup>1</sup>, Jianxun Wang<sup>1</sup>, Qi Huang<sup>1</sup>, Jiawei Hu<sup>1</sup>,  
10 Rong Zeng<sup>2,\*</sup>, Bian Wu<sup>2,\*</sup>

11  
12 <sup>1</sup>Department of Gastrointestinal and Bariatric Metabolic Surgery, The First People's Hospital of  
13 Yunnan Province, The Affiliated Hospital of Kunming University of Science and Technology,  
14 Kunming, Yunnan, China; <sup>2</sup>Department of Medical Oncology, The First People's Hospital of  
15 Yunnan Province, The Affiliated Hospital of Kunming University of Science and Technology,  
16 Kunming, Yunnan, China

17  
18 \*Correspondence: [rongzi2005146@163.com](mailto:rongzi2005146@163.com); [wubian666888@sina.com](mailto:wubian666888@sina.com)

19  
20 **Received November 27, 2025 / Accepted April 20, 2026**

21  
22 Chromosome instability (CIN) is a major contributor to drug resistance and recurrence. As a crucial  
23 mechanism of CIN, centrosome clustering has emerged as a promising therapeutic strategy.  
24 However, the roles and regulatory mechanisms of centrosome clustering in gastric cancer remain  
25 unclear. BATF2 was previously identified as a key modulator of multidrug resistance (MDR) in  
26 gastric cancer (GC). To examine the involvement of centrosome clustering in the mechanism by  
27 which BATF2 reverses MDR in GC, adriamycin (ADR)- and vincristine (VCR)-resistant cell lines,  
28 NCI-N87/ADR and NCI-N87/VCR, were used for investigations. Expression of BATF2 was  
29 downregulated in both drug-resistant cells, particularly in NCI-N87/ADR cells. Cells with BATF2  
30 knockdown exhibited higher cell viability and lower apoptosis rates, and such changes were  
31 reversed by BATF2 overexpression. The enhanced centrosome clustering in cells transfected with  
32 sh-BATF2 was accompanied by increased KIFC1 expression, which was inhibited after BATF2  
33 overexpression. BATF2 reversed MDR and inhibited centrosome clustering by inhibiting ATM  
34 phosphorylation, which was evidenced by ATM overexpression. Meanwhile, KU-60019, a specific  
35 inhibitor of ATM, could markedly reverse the pro-tumor effects of BATF2 knockdown. In  
36 conclusion, BATF2 is a potential target for reversing MDR in GC, and targeting KIFC1-related  
37 centrosome clustering by suppressing ATM phosphorylation is proposed as a key mechanism.

38  
39 **Key words:** gastric cancer; multidrug resistance; centrosome clustering; BATF2

40  
41  
42 Gastric cancer (GC) is a malignancy originating from gastric mucosal epithelium [1]. Global Cancer  
43 Statistics estimate that GC is the fifth leading cause of both cancer incidence and cancer-related  
44 deaths worldwide, with 968,350 newly diagnosed GC cases (4.9% of all new cases) and 659,853

45 GC-caused deaths (6.8% of all cancer-related deaths) in 2022 [2]. Treatment options for GC depend  
46 primarily on the stage of the disease at the time of presentation, but most patients are seen at an  
47 advanced stage and require pharmacotherapy, mainly chemotherapy [3]. Conventional  
48 chemotherapeutics comprises of cisplatin, epirubicin, paclitaxel and 5-fluorouracil. Nevertheless,  
49 the 5-year overall survival rate for GC remains below 30% because of limited curative effect of  
50 chemotherapy [4]. Although chemotherapy drugs have continued to advance over the past few years,  
51 improving survival outcomes for patients with advanced GC, progress has reached a bottleneck [5,  
52 6]. The main reason is that GC cells develop multidrug resistance (MDR), which leads to reduced  
53 sensitivity to chemotherapy [1, 7, 8]. Therefore, identifying methods to reverse MDR clinically and  
54 improve chemotherapy efficacy has become a focal point and a challenge in current research.

55 Mounting evidence suggests that the MDR mechanism of GC is closely related to chromosomal  
56 instability (CIN) abnormalities [9, 10]. CIN is widely recognized as a hallmark of tumors [11],  
57 including GC, and is positively associated with treatment resistance, poor clinical outcomes,  
58 immune evasion, and a high risk of recurrence and metastasis [12, 13]. Whereas CIN usually  
59 exhibits centrosome amplification [14, 15], and to avoid multipolar spindles and cell death, cancer  
60 cells achieve bipolar division by inducing supernumerary centrosome clustering, an adaptive  
61 survival strategy that allows cancer cells to divide successfully despite bearing supernumerary  
62 centrosomes [15, 16]. As a crucial mechanism of CIN, centrosome clustering has been proposed as  
63 a promising target for therapeutic intervention of human cancers [17, 18]. Nevertheless, the  
64 regulatory mechanisms of centrosome clustering and functions of centrosome clustering remain  
65 largely unclear.

66 Kinesin Family Member C1 (KIFC1) is a novel driver protein and centrosome clustering regulator  
67 participating in extra centrosome clustering in tumor cells [16, 19]. Elevated expression of KIFC1  
68 has been observed in GC tissues [20], and its high expression is linked to a worse clinical outcome  
69 [21, 22]. KIFC1 knockdown could repress the sphere formation of GC cells, indicating the close  
70 involvement of KIFC1 in GC stem cells [20]. In addition, KIFC1 mediates the resistance to drugs,  
71 such as docetaxel [23] and cisplatin [24] in other cancers. However, whether KIFC1 mediates MDR  
72 of GC cells, and the associations between its functions and centrosome clustering in GC, have not  
73 been reported in GC.

74 Basic Leucine Zipper ATF-Like Transcription Factor 2 (BATF2), also termed SARI, has been

75 recognized as a novel tumor suppressor in human tumors [25-27]. In GC, Xie et al. demonstrate that  
76 reduced BATF2 expression in GC tissues is linked to peritoneal recurrence post-curative  
77 gastrectomy, and that GC growth and metastasis can be restrained by enhancing BATF2 expression  
78 [28]. Our previous studies have demonstrated the important role of BATF2 in reversing MDR and  
79 inhibiting chemotherapy resistance in GC [29-31]. However, whether BATF2 regulates centrosome  
80 clustering and thus affects the mechanism of MDR in GC remains unknown. To address this issue,  
81 we conducted the current study to elucidate the possible linkages among BATF2, centrosome  
82 clustering and MDR in GC based on two MDR cell models. This study may provide novel insights  
83 to illustrate the mechanism of MDR in GC.

84

## 85 **Materials and Methods**

86 **Establishment of drug-resistant cells.** GC cell line NCI-N87 from Wuhan Procell Life Technology  
87 Co., LTD. (#CL-0169, China) was maintained in RPMI-1640 medium bearing an additional adding  
88 of 10% FBS (#16140071, Gibco) and 1% penicillin-streptomycin under the conditions of 5% CO<sub>2</sub>  
89 at 37 °C. Adriamycin (ADR, #A864033, Macklin, Shanghai, China) and Vincristine (VCR,  
90 #V861369, Macklin)-resistant cells, NCI-N87/ADR and NCI-N87/VCR, were acquired via  
91 enhancing drug dose gradually as previously described [32-34]. For the culture of drug-resistant  
92 cells, a final concentration of 0.5 mg/mL ADR and 1 mg/mL VCR was used to maintain the  
93 drug-resistant phenotype.

94 **Cell transfection.** Lentiviral vector system was employed to overexpress BATF2 and  
95 ataxia-telangiectasia mutated (ATM) or to knockdown BATF2. Based on DSIR website  
96 (<http://biodev.cea.fr/DSIR/>), we designed short hairpin RNA (shRNA) against BATF2:  
97 5'-ACACTATGTTAGTATCTAA-3' (sense), and 5'-ACACTATGTTAGTATCTAA-3' (antisense).  
98 From NCBI database, we retrieved sequences of mature BATF2 and ATM. Subsequently, we  
99 transfected vectors bearing sh-BATF2, BATF2, ATM as well as matching (negative control) NC  
100 sequences into 293T cells, along with the packaging plasmids (pMDLg/pRRE: pVSV-G:  
101 pRSV-Rev=5:3:2) with the aids of HighGene reagent, followed by collecting and concentrating  
102 lentivirus particles 48h after transfection. For lentiviral infection, NCI-N87/ADR and  
103 NCI-N87/VCR cells ( $1 \times 10^5$ /ml) were inoculated into 6-well plates, and lentivirus ( $1 \times 10^8$  TU/ml)  
104 was added to the medium at 70-90% confluency. Following 48 h post-infection, 2.5 µg/ml

105 puromycin was added to select stably transfected cells.

106 **qRT-PCR.** Total RNAs isolation from cells were conducted with the aids of TRIzol reagent  
107 (#15596018, Invitrogen). The isolated RNAs were reversely transcribed into cDNA using FastKing  
108 RT SuperMix (#KR118-02, TIANGEN), followed by PCR amplification with the aids of SYBR  
109 Green PCR Master Mix (#A4004M, Lifeint). The used primers are: BATF2-F:  
110 5'-GCTCCTGTGGGCAAGAGAAT-3'; BATF2-R: 5'-AGAGAGCAGGTTTGTGCTCC-3';  
111 GAPDH-F: 5'- CCATGGGGAAGGTGAAGGTC-3'; GAPDH-R: 5'-  
112 AGTGATGGCATGGACTGTGG-3'.

113 **Western blot.** After cell lysis with RIPA, concentration of cell proteins was determined with the  
114 aids of BCA assay kit. Proteins were separated, transferred onto PVDF membranes, followed by  
115 incubation with antibodies BATF2 (#PA5-103647, Thermo), anti-KIFC1 (#12313, CST), anti-ATM  
116 (#2873, CST) and anti-phosphorylated ATM (p-ATM, #5883, CST) overnight at 4 °C. Secondary  
117 antibodies incubation was then carried out for 60 min at dark. The blotting bands were washed by  
118 ECL reagent and were packaged using a cling film, and were transferred to cassette for film  
119 exposure.

120 **Immunofluorescence.** Immunofluorescence was performed according to the methods in previous  
121 studies. In brief, cells were re-suspended into a 12-well plate containing cell sliver, and were treated  
122 with ADR or VCR for 24 h. After cell fixation, permeabilization and blocking, anti- $\alpha$ -tubulin and  
123 anti-centrin-2 were added to incubate with cells overnight at 4 °C. Afterwards, IgG H&L (Alexa  
124 Fluor® 647) secondary antibody incubation and DAPI staining were carried out. Finally, sections  
125 were scanned on a laser scanning confocal microscope after sealed with fluorescent quenching  
126 sealant.

127 **CCK-8 assay.** Cells were placed in 96-well plates (2,000 cells/well), and were treated with ADR or  
128 VCR. After 24 h of treatment, 10  $\mu$ l CCK-8 was added to each well for 2 h to calculate the cell  
129 counts on the basis of the optical density at 450 nm.

130 **Flow cytometry (FCM).** Apoptosis was determined using an Annexin V-FITC apoptosis kit  
131 (#C1062S, Beyotime). Briefly, after digested with 0.25% EDTA-free Tyrisin, cells were collected  
132 by centrifugation. Then, cells were washed by pre-cooled PBS and were resuspended in 300  $\mu$ l  
133 binding Buffer, followed by incubation with 5  $\mu$ l Annexin V-FITC and 10  $\mu$ l of propidium iodide in  
134 dark. The cells were analyzed by an CytoFLEX S FCM (Beckman Coulter Life Sciences, USA),

135 and were analyzed using CELL Quest software.

136 **Co-Immunoprecipitation (Co-IP).** To explore the interaction between BATF2 and ATM, we  
137 conducted Co-IP assay according to the manual of the rProtein A/G Magnetic IP/Co-IP Kit  
138 (#abs9649, absin). Briefly, cells were collected and washed by PBS, and then were lysed in 1x  
139 Lysis/Wash Buffer (Enhanced) on ice. After centrifugation at  $14,000 \times g$ ,  $4^\circ C$  for 10 min, the  
140 supernatant was collected, and was precleared with protein A/G beads for 2 h before incubation  
141 with primary antibodies: anti-ATM (#16592-1-AP, Proteintech) and anti-BATF2 (#16592-1-AP,  
142 Proteintech). Isotype immunoglobulin G (IgG) antibody was used as negative control. Afterwards,  
143 Protein A/G MagPoly Beads were added to the immunoprecipitation mixture and rotated for 30 min.  
144 Afterwards, the immunoprecipitated protein complexes were washed with Elution buffer, and the  
145 resulting supernatants were collected, and Neutralization Buffer was added. Finally, the collected  
146 supernatants were detected by Western blot.

147 **Statistical analysis.** All experiments were conducted with three repetitions. Data presenting in the  
148 form of mean $\pm$ standard deviation was employed for statistics. Data for changes on cell viability  
149 along with the drug dosages was compared by two-way RM ANOVA. ANOVA coupled a Tukey's  
150 post hoc test was employed for statistics of other data.  $P < 0.05$  denotes statistical difference.

## 152 Results

153 **BATF2 overexpression enhances susceptibility of NCI-N87 cells to ADR and VCR.** Expression  
154 of BATF2 was detected in drug-resistant cells: NCI-N87/ADR and NCI-N87/VCR. Compared with  
155 that in NCI-N87 cells, significant decrease in its protein expression was observed in these two  
156 drug-resistant cells, particularly in NCI-N87/ADR cells (Figure 1A). To elucidate the exact roles of  
157 BATF2 expression in MDR, we first established BATF2 overexpression or knockdown model in  
158 NCI-N87/ADR and NCI-N87/VCR cells (Figure 1B). Subsequently, cell viability was determined  
159 using the CCK-8 assay, and we found that BATF2 overexpression exhibited enhanced  
160 chemosensitivity (low cell viability) to ADR and VCR than matched NC group. Cells with BATF2  
161 knockdown showed highest cell viability, indicating that BATF2 knockdown decreased  
162 susceptibility to ADR and VCR (Figure 1C). Consistently, FCM analysis indicated that in two  
163 drug-resistant cells, BATF2 overexpression exhibited highest apoptosis rate, whereas BATF2  
164 knockdown exhibited lowest apoptosis rate (Figures 1D, 1E). All these results suggest that BATF2

165 inhibition promotes MDR, while BATF2 overexpression sensitizes NCI-N87 cells to chemotherapy.  
166 **BATF2 overexpression inhibits KIFC1 expression and centrosome clustering.** KIFC1 is a  
167 centrosome clustering molecule that prevents cancer cells from undergoing  
168 centrosome-amplification-induced apoptosis [35]. We found that expression of KIFC1 was  
169 markedly reduced in NCI-N87/ADR and NCI-N87/VCR cells with BATF2 overexpression, whereas  
170 KIFC1 expression was observably enhanced in NCI-N87/ADR and NCI-N87/VCR cells with  
171 BATF2 knockdown (Figure 2A). Centrosome clustering was further observed by  
172 immunofluorescence staining. As shown in (Figure 2B), ratio of centrosome clustering was high in  
173 cells with BATF2 knockdown in comparison with corresponding NC. After BATF2 overexpression,  
174 the ratio of centrosome clustering significant decreased. Similar results were also observed in  
175 NCI-N87/VCR cells (Figure 2B).

176 **BATF2 overexpression inhibits the elevated p-ATM in drug-resistant cells.** Expression of ATM  
177 and p-ATM was determined, and we found that compared with NCI-N87 cells, the drug-resistant  
178 NCI-N87/ADR and NCI-N87/VCR cells showed markedly elevated level of p-ATM, particularly in  
179 NCI-N87/ADR cells (Figure 3A). To investigate the possible interaction between BATF2 and ATM,  
180 we conducted Co-IP assay. The results indicated that BATF2 and ATM were co-precipitated with  
181 each other (Figure 3B), suggesting that BATF2 could directly interact with ATM. Besides, in both  
182 NCI-N87/ADR and NCI-N87/VCR cells, BATF2 overexpression could significantly reduce the  
183 level of p-ATM, while BATF2 knockdown could elevate p-ATM level in drug-resistant cells (Figure  
184 3C). These results suggested that p-ATM level was increased in multidrug-resistant NCI-N87 cells,  
185 and such increased p-ATM level could be inhibited by BATF2 overexpression.

186 **BATF2 mediates chemosensitivity and centrosome clustering by inhibiting p-ATM.** To  
187 validation whether ATM involving in the actions of BATF2-mediated chemosensitivity, we further  
188 overexpressed ATM in BATF2-overexpressed multidrug-resistant NCI-N87 cells. ATM  
189 overexpression showed no influences on the expression of BATF2 (Figure 4A). BATF2  
190 overexpression could significantly reduce the level of p-ATM/ATM, while such decrease could be  
191 partly reversed following ATM overexpression (Figure 4A). BATF2 overexpression exhibited  
192 enhanced chemosensitivity (lower cell viability and higher cells apoptosis) to ADR and VCR than  
193 matched NC group, and such susceptibility was partly reversed following ATM overexpression  
194 (Figures 4B, 4C). Moreover, overexpression of ATM elevated the reduced KIFC1 and reduced ratio

195 of centrosome clustering caused by BATF2 overexpression in both NCI-N87/ADR and  
196 NCI-N87/VCR cells (Figures 5A, 5B). Meanwhile, 3  $\mu$ M KU-60019 (#Y242876, Beyotime), a  
197 specific inhibitor of ATM, was used to inhibit ATM in cells with BATF2 knockdown. As expected,  
198 KU-60019 treatment markedly reduced the increased level of p-ATM/ATM caused by BATF2  
199 knockdown in both two cells (Figure 6A). In addition, BATF2 knockdown observably promoted  
200 cells viability (Figure 6B) and inhibited cell apoptosis (Figure 6C), while such effects of BATF2  
201 knockdown were markedly reversed after KU-60019 treatment (Figures 6B, 6C). Altogether, these  
202 findings suggested that BATF2 could mediate chemosensitivity and centrosome clustering by  
203 inhibiting p-ATM.

204

## 205 **Discussion**

206 Although chemotherapy can prolong the survival of patients with advanced GC, the overall survival  
207 rate is still not ideal. MDR is the primary factor that limits the therapeutic effect of chemotherapy  
208 and leads to the death of patients [36, 37]. CIN is one of the main features of solid tumors, including  
209 GC, and has been demonstrated to contribute to the therapeutic resistance in cancer treatment [38,  
210 39]. Although CIN is a feature of GC [40], centrosome clustering, a contributor to CIN, has not  
211 been reported in GC, especially its relationship with MDR in GC.

212 The centrosome is the primary microtubule-organizing center, which ensures the symmetry and  
213 bipolarity of cell division by establishing bipolar spindle; this function is essential for accurate cell  
214 mitosis [18]. Unlike normal cells, cancer cells often exhibit supernumerary centrosomes, called  
215 centrosome amplification, which is a hallmark of cancer and is strongly associated with tumor  
216 progression, poor clinical outcomes, and multiple carcinogenic phenotypes, such as aneuploidy [41].  
217 For cancer cells with supernumerary centrosomes, to avoid the emergence of multiple spindles that  
218 can trigger cell death, cancer cells usually achieve pseudo-bipolar division by centrosome clustering  
219 to form pseudo-bipolar spindles, thus ensuring cell survival, which is an adaptive survival  
220 mechanism of tumor cells [42, 43]. Therefore, targeting centrosome clustering may be a promising  
221 therapeutic strategy, and understanding the processes that control centrosome clustering is crucial  
222 for this strategy. In this study, we found that overexpression of BATF2 not only inhibited the  
223 supernumerary centrosomes clustering, but also reduced cell viability and increased apoptosis of  
224 both NCI-N87/ADR and NCI-N87/VCR cells, possibly due to the induction of multipolar division.

225 The results of this study emphasize the involvement of centrosome clustering in MDR, and  
226 targeting centrosomes clustering may enhance the sensitivity to chemotherapeutics.

227 KIFC1 has recently been recognized as centrosome clustering molecule, which is fundamental for  
228 viability of tumor cells bearing supernumerary centrosome [16, 44]. Specifically, KIFC1 allows  
229 tumor cells bearing multiple centrosomes to survive cell division, which is not necessary for normal  
230 somatic cells, but is necessary for normal division in tumor cells bearing supernumerary  
231 centrosomes [45, 46]. The loss of KIFC1 could cause death of tumor cells by inducing deadly  
232 multipolar division, but no influence was observed for the division of normal cells possessing two  
233 centrosomes [47]. Expression of KIFC1 was found to be up-regulated in GC tissues [21], and its  
234 enhanced expression was strongly linked to lymph node/distant metastasis, depth of invasion, TNM  
235 stage, tumor size and a worse survival in GC [22]. Hence, KIFC1 suppression is proposed as an  
236 available strategy to for GC treatment. In this study, we found that expression of KIFC1 was  
237 elevated in both ADR and VCR-resistant GC cell lines, and such elevated expression could be  
238 markedly reduced after BATF2 overexpression, accompanied by a decrease in the number of cells  
239 with centrosome clustering. The cooccurrence of KIFC1 dysregulation with centrosome clustering  
240 suggests that targeting KIFC1 might be an available strategy to modulate centrosome clustering.

241 BATF2, a transcription factor of bZIP family, has been reported to participate in the progression of a  
242 wide variety of human cancers. Particularly, BATF2 exerts as a tumor suppressor, and its high level  
243 is frequently associated with an inhibition of tumor growth and metastasis [25, 48-52]. In GC,  
244 BATF2 expression was reduced in GC tissues [28]. Such reduced BATF2 expression in GC showed  
245 correlations with a worse survival outcome and stem cell-like properties, and enhanced BATF2  
246 level was linked to an increased responsiveness to 5-Fluorouracil and an improved outcomes of GC  
247 patients who received postoperative chemotherapy [53]. In terms of mechanism, BATF2 was found  
248 to inhibit drug transporter ABCG2 and to inhibit AKT phosphorylation while promote PTEN  
249 stability [53]. In previous studies [29-31], we investigated the functional roles and the underlying  
250 mechanisms of BATF2 in GC MDR cells, and found that it can reverse MDR through decreasing  
251 P-glycoprotein (P-gp, an ABC transporter) mediated drug efflux via inhibiting AP-1 [29] or  
252 Wnt/ $\beta$ -catenin signaling [30], or through inhibiting Drp1-dependent mitochondrial fission via  
253 p53/ERK pathway in GC [31]. In this study, we found that BATF2 could reverse MDR and inhibit  
254 KIFC1-mediated centrosome clustering by inhibiting p-ATM *in vitro*. Consistently, a previous study

255 also revealed the regulatory roles of ATM kinases on centrosome clustering [46]. ATM kinase is a  
256 key protein that is frequently recruited and activated in DNA damage response (DDR) pathway to  
257 trigger cell cycle arrest and promote DNA repair [54]. DDR defect is an established driver and  
258 hallmark of cancers, and the activation of ATM in DDR pathway is found to be benefits for  
259 abnormal cell survival [54]. Through the autophosphorylation at Ser1981, ATM modulates the  
260 cellular responses to DNA double-strand breaks [55]. p-ATM was observed to be elevated in  
261 drug-resistant NCI-N87/ADR and NCI-N87/VCR cells, and such enhanced p-ATM level could be  
262 inhibited after BATF2 overexpression. The possible mechanism by which overexpression of BATF2  
263 reverses MDR in GC cells has been summarized in Figure 7. These results indicated that BATF2  
264 could target KIFC1-related centrosome clustering by suppressing p-ATM, thus enhancing the  
265 chemosensitivity of GC cells to VCR and ADR. This study broadens our understanding of the  
266 mechanism of BATF2 in MDR in GC, and contributes to the translational feasibility of BATF2 in  
267 GC.

268 Limitations and prospects: Although this study demonstrated the role of BATF2 in reversing MDR  
269 of GC cells to VCR and ADR by inhibiting KIFC1-mediated centrosome clustering, whether  
270 KIFC1-mediated centrosome clustering is involved in resistance of GC cells to other  
271 chemotherapeutics is largely unclear, and this should be investigated in future studies. In addition,  
272 our results suggest that ATM positively regulates KIFC1 as a downstream of BATF2, and ATM can  
273 reverse the inhibitory effects of BATF2 on KIFC1. However, it is not yet clear whether ATM  
274 regulates KIFC1 at the transcriptional level or the protein level, and this will be investigated in our  
275 subsequent studies. Besides, a previous study indicated that expression of BATF2 showed close  
276 linkage with infiltration of activated CD4<sup>+</sup> memory T cells, and the signature based on  
277 CD36-BATF2/MYB could be used as an indicator for predicting the response to anti-PD-1  
278 immunotherapy [56]. Li et al. [57] observed upregulated expression of PD-L1 in GC MKN-45 cells  
279 with BATF2 knockdown, indicating the potential of BATF2 as a biomarker for predicting the  
280 efficacy of PD-L1 blockade therapy in GC. Therefore, whether BATF2 mediates the sensitivity of  
281 GC cells to immune checkpoint blockade therapy should also be investigated in future studies.  
282 Finally, *in vivo* validation should be conducted in our future investigations to strengthen the  
283 reliability and translational value of this study.

284 In summary, this study demonstrated that centrosome clustering existed in MDR GC cells. BATF2

285 overexpression could inhibit cell viability, centrosome clustering and KIFC1 expression, while  
286 induce apoptosis in NCI-N87/ADR and NCI-N87/VCR cells. We proposed that BATF2 could  
287 reverse MDR in GC cells and inhibit KIFC1-mediated centrosome clustering via inhibiting p-ATM.  
288 This study provided a new perspective on the mechanism by which BATF2 reverses MDR in GC.

289  
290 Acknowledgements: This work was supported by Co-operation Fund of Kunming Medical  
291 University and the Science and Technology Department of Yunnan Province (grant number  
292 202301AY070001-63), Beijing Science And Technology Innovation Medical Development  
293 Foundation (grant number KC2023-JX-0186-FZ095) and Yunnan Provincial Department of Science  
294 and Technology-Major Science and Technology Special Project Plan of Yunnan Province  
295 Biomedical and Health Industry Promotion Center (grant number 202402AA310006).

## 298 **References**

- 299 [1] LIU J, YUAN Q, GUO H, GUAN H, HONG Z et al. Deciphering drug resistance in gastric  
300 cancer: Potential mechanisms and future perspectives. *Biomed Pharmacother* 2024; 173:  
301 116310. <https://doi.org/10.1016/j.biopha.2024.116310>
- 302 [2] BRAY F, LAVERSANNE M, SUNG H, FERLAY J, SIEGEL RL et al. Global cancer  
303 statistics 2022: GLOBOCAN estimates of incidence and mortality worldwide for 36 cancers  
304 in 185 countries. *CA Cancer J Clin* 2024; 74: 229-263. <https://doi.org/10.3322/caac.21834>
- 305 [3] GUAN WL, HE Y, XU RH. Gastric cancer treatment: recent progress and future  
306 perspectives. *J Hematol Oncol* 2023; 16: 57. <https://doi.org/10.1186/s13045-023-01451-3>
- 307 [4] WANG G, HUANG Y, ZHOU L, YANG H, LIN H et al. Immunotherapy and targeted  
308 therapy as first-line treatment for advanced gastric cancer. *Crit Rev Oncol Hematol* 2024;  
309 198: 104197. <https://doi.org/10.1016/j.critrevonc.2023.104197>
- 310 [5] SMYTH EC, NILSSON M, GRABSCH HI, VAN GRIEKEN NC, LORDICK F. Gastric  
311 cancer. *Lancet* 2020; 396: 635-648. [https://doi.org/10.1016/s0140-6736\(20\)31288-5](https://doi.org/10.1016/s0140-6736(20)31288-5)
- 312 [6] LI K, ZHANG A, LI X, ZHANG H, ZHAO L. Advances in clinical immunotherapy for  
313 gastric cancer. *Biochim Biophys Acta Rev Cancer* 2021; 1876: 188615.  
314 <https://doi.org/10.1016/j.bbcan.2021.188615>
- 315 [7] CHE G, YIN J, WANG W, LUO Y, CHEN Y et al. Circumventing drug resistance in gastric  
316 cancer: A spatial multi-omics exploration of chemo and immuno-therapeutic response  
317 dynamics. *Drug Resist Updat* 2024; 74: 101080. <https://doi.org/10.1016/j.drup.2024.101080>
- 318 [8] ZHOU Y, CHEN Y, SHI Y, WU L, TAN Y et al. FAM117B promotes gastric cancer growth  
319 and drug resistance by targeting the KEAP1/NRF2 signaling pathway. *J Clin Invest* 2023;  
320 133: e158705. <https://doi.org/10.1172/jci158705>
- 321 [9] LUKOW DA, SHELTZER JM. Chromosomal instability and aneuploidy as causes of cancer  
322 drug resistance. *Trends Cancer* 2022; 8: 43-53. <https://doi.org/10.1016/j.trecan.2021.09.002>

- 323 [10] LUKOW DA, SAUSVILLE EL, SURI P, CHUNDURI NK, WIELAND A et al.  
324 Chromosomal instability accelerates the evolution of resistance to anti-cancer therapies. *Dev*  
325 *Cell* 2021; 56: 2427-39.e4. <https://doi.org/10.1016/j.devcel.2021.07.009>
- 326 [11] DREWS RM, HERNANDO B, TARABICHI M, HAASE K, LESLUYES T et al. A  
327 pan-cancer compendium of chromosomal instability. *Nature* 2022; 606: 976-983.  
328 <https://doi.org/10.1038/s41586-022-04789-9>
- 329 [12] BAKHOUM SF, CANTLEY LC. The Multifaceted Role of Chromosomal Instability in  
330 Cancer and Its Microenvironment. *Cell* 2018; 174: 1347-1360.  
331 <https://doi.org/10.1016/j.cell.2018.08.027>
- 332 [13] CHEN X, AGUSTINUS AS, LI J, DIBONA M, BAKHOUM SF. Chromosomal instability  
333 as a driver of cancer progression. *Nat Rev Genet* 2025; 26: 31-46.  
334 <https://doi.org/10.1038/s41576-024-00761-7>
- 335 [14] PIEMONTE KM, ANSTINE LJ, KERI RA. Centrosome Aberrations as Drivers of  
336 Chromosomal Instability in Breast Cancer. *Endocrinology* 2021; 162: bqab208.  
337 <https://doi.org/10.1210/endocr/bqab208>
- 338 [15] KRÄMER A, MAIER B, BARTEK J. Centrosome clustering and chromosomal (in)stability:  
339 a matter of life and death. *Mol Oncol* 2011; 5: 324-335.  
340 <https://doi.org/10.1016/j.molonc.2011.05.003>
- 341 [16] MAROTTA VE, SABAT-POŚPIECH D, FIELDING AB, PONSFORD AH, THOMAZ A et  
342 al. OTUD6B regulates KIFC1-dependent centrosome clustering and breast cancer cell  
343 survival. *EMBO Rep* 2025; 26: 1003-1035. <https://doi.org/10.1038/s44319-024-00361-w>
- 344 [17] GODINHO SA, KWON M, PELLMAN D. Centrosomes and cancer: how cancer cells  
345 divide with too many centrosomes. *Cancer Metastasis Rev* 2009; 28: 85-98.  
346 <https://doi.org/10.1007/s10555-008-9163-6>
- 347 [18] FIRDOUS F, RAZA HG, CHOTANA GA, CHOUDHARY MI, FAISAL A et al. Centrosome  
348 Clustering & Chemotherapy. *Mini Rev Med Chem* 2023; 23: 429-451.  
349 <https://doi.org/10.2174/1389557522666220820113953>
- 350 [19] ZHANG C, WU BZ, DI CIANO-OLIVEIRA C, WU YF, KHAVKINE BINSTOCK SS et al.  
351 Identification of KIFC1 as a putative vulnerability in lung cancers with centrosome  
352 amplification. *Cancer Gene Ther* 2024; 31: 1559-1570.  
353 <https://doi.org/10.1038/s41417-024-00824-1>
- 354 [20] OUE N, MUKAI S, IMAI T, PHAM TT, OSHIMA T et al. Induction of KIFC1 expression in  
355 gastric cancer spheroids. *Oncol Rep* 2016; 36: 349-355.  
356 <https://doi.org/10.3892/or.2016.4781>
- 357 [21] CAO FY, ZHENG YB, YANG C, HUANG SY, HE XB et al. miR-635 targets KIFC1 to  
358 inhibit the progression of gastric cancer. *J Investig Med* 2020; 68: 1357-1363.  
359 <https://doi.org/10.1136/jim-2020-001438>
- 360 [22] JUNG J, JEONG H, CHOI JW, KIM HS, OH HE et al. Increased expression levels of  
361 AURKA and KIFC1 are promising predictors of progression and poor survival associated  
362 with gastric cancer. *Pathol Res Pract* 2021; 224: 153524.  
363 <https://doi.org/10.1016/j.prp.2021.153524>
- 364 [23] SEKINO Y, OUE N, KOIKE Y, SHIGEMATSU Y, SAKAMOTO N et al. KIFC1 Inhibitor  
365 CW069 Induces Apoptosis and Reverses Resistance to Docetaxel in Prostate Cancer. *J Clin*  
366 *Med* 2019; 8: 225. <https://doi.org/10.3390/jcm8020225>

- 367 [24] GAO H, WANG J, LIU J, WANG H, WANG T et al. FOXD1 activates KIFC1 to modulate  
368 aerobic glycolysis and reinforce cisplatin resistance of breast cancer. *Reprod Biol* 2025; 25:  
369 100969. <https://doi.org/10.1016/j.repbio.2024.100969>
- 370 [25] ZHANG X, LIU Y, DAI L, SHI G, DENG J et al. BATF2 prevents glioblastoma multiforme  
371 progression by inhibiting recruitment of myeloid-derived suppressor cells. *Oncogene* 2021;  
372 40: 1516-1530. <https://doi.org/10.1038/s41388-020-01627-y>
- 373 [26] ZHOU J, LEI Z, CHEN J, LIAO S, CHEN Y et al. Nuclear export of BATF2 enhances  
374 colorectal cancer proliferation through binding to CRM1. *Clin Transl Med* 2023; 13: e1260.  
375 <https://doi.org/10.1002/ctm2.1260>
- 376 [27] HAN T, WANG Z, YANG Y, SHU T, LI W et al. The tumor-suppressive role of BATF2 in  
377 esophageal squamous cell carcinoma. *Oncol Rep* 2015; 34: 1353-1360.  
378 <https://doi.org/10.3892/or.2015.4090>
- 379 [28] XIE JW, HUANG XB, CHEN QY, MA YB, ZHAO YJ et al. m(6)A modification-mediated  
380 BATF2 acts as a tumor suppressor in gastric cancer through inhibition of ERK signaling.  
381 *Mol Cancer* 2020; 19: 114. <https://doi.org/10.1186/s12943-020-01223-4>
- 382 [29] YANG W, ZHAO S, WU B, XU J, WU Z et al. BATF2 inhibits chemotherapy resistance by  
383 suppressing AP-1 in vincristine-resistant gastric cancer cells. *Cancer Chemother Pharmacol*  
384 2019; 84: 1279-1288. <https://doi.org/10.1007/s00280-019-03958-4>
- 385 [30] YANG W, WU B, MA N, WANG Y, GUO J et al. BATF2 reverses multidrug resistance of  
386 human gastric cancer cells by suppressing Wnt/ $\beta$ -catenin signaling. *In Vitro Cell Dev Biol*  
387 *Anim* 2019; 55: 445-452. <https://doi.org/10.1007/s11626-019-00360-5>
- 388 [31] YANG W, ZENG R, SONG J, MAN, ZHU W et al. Drp1-Dependent Mitochondrial Fission  
389 is Involved in Adriamycin Resistance in Gastric Cancer Cells: A Perspective from the  
390 BATF2/p53/ERK Regulatory Axis. *Tohoku J Exp Med* 2025.  
391 <https://doi.org/10.1620/tjem.2025.J091>
- 392 [32] WANG S, CHEN W, YU H, SONG Z, LI Q et al. lncRNA ROR Promotes Gastric Cancer  
393 Drug Resistance. *Cancer Control* 2020; 27: 1073274820904694.  
394 <https://doi.org/10.1177/1073274820904694>
- 395 [33] TRAVERSO N, RICCIARELLI R, NITTI M, MARENGO B, FURFARO AL et al. Role of  
396 glutathione in cancer progression and chemoresistance. *Oxid Med Cell Longev* 2013; 2013:  
397 972913. <https://doi.org/10.1155/2013/972913>
- 398 [34] LI DQ, WANG ZB, BAI J, ZHAO J, WANG Y et al. Reversal of multidrug resistance in  
399 drug-resistant human gastric cancer cell line SGC7901/VCR by antiprogestin drug  
400 mifepristone. *World J Gastroenterol* 2004; 10: 1722-1725.  
401 <https://doi.org/10.3748/wjg.v10.il2.1722>
- 402 [35] JINNA N, YUAN YC, RIDA P. Kinesin Family Member C1 (KIFC1/HSET) Underlies  
403 Aggressive Disease in Androgen Receptor-Low and Basal-Like Triple-Negative Breast  
404 Cancers. *Int J Mol Sci* 2023; 24: 16072. <https://doi.org/10.3390/ijms242216072>
- 405 [36] WANG J, HUANG Q, HU X, ZHANG S, JIANG Y et al. Disrupting Circadian Rhythm via  
406 the PER1-HK2 Axis Reverses Trastuzumab Resistance in Gastric Cancer. *Cancer Res* 2022;  
407 82: 1503-1517. <https://doi.org/10.1158/0008-5472.Can-21-1820>
- 408 [37] HU X, MA Z, XU B, LI S, YAO Z et al. Glutamine metabolic microenvironment drives M2  
409 macrophage polarization to mediate trastuzumab resistance in HER2-positive gastric cancer.  
410 *Cancer Commun (Lond)* 2023; 43: 909-937. <https://doi.org/10.1002/cac2.12459>

- 411 [38] PANCIONE M, CERULO L, REMO A, GIORDANO G, GUTIERREZ-UZQUIZA Á et al.  
412 Centrosome Dynamics and Its Role in Inflammatory Response and Metastatic Process.  
413 *Biomolecules* 2021; 11: 629. <https://doi.org/10.3390/biom11050629>
- 414 [39] SANSREGRET L, VANHAESEBROECK B, SWANTON C. Determinants and clinical  
415 implications of chromosomal instability in cancer. *Nat Rev Clin Oncol* 2018; 15: 139-150.  
416 <https://doi.org/10.1038/nrclinonc.2017.198>
- 417 [40] CHEN Z, ZHANG C, ZHANG M, LI B, NIU Y et al. Chromosomal instability of circulating  
418 tumor DNA reflect therapeutic responses in advanced gastric cancer. *Cell Death Dis* 2019;  
419 10: 697. <https://doi.org/10.1038/s41419-019-1907-4>
- 420 [41] SAATCI O, AKBULUT O, CETIN M, SIKIRZHYTSKI V, UNER M et al. Targeting  
421 TACC3 represents a novel vulnerability in highly aggressive breast cancers with centrosome  
422 amplification. *Cell Death Differ* 2023; 30: 1305-1319.  
423 <https://doi.org/10.1038/s41418-023-01140-1>
- 424 [42] KALKAN BM, OZCAN SC, CICEK E, GONEN M, ACILAN C. Nek2A prevents  
425 centrosome clustering and induces cell death in cancer cells via KIF2C interaction. *Cell*  
426 *Death Dis* 2024; 15: 222. <https://doi.org/10.1038/s41419-024-06601-0>
- 427 [43] MASHIMA Y, NOHIRA H, SUGIHARA H, DYNLACHT BD, KOBAYASHI T et al. KIF24  
428 depletion induces clustering of supernumerary centrosomes in PDAC cells. *Life Sci Alliance*  
429 2022; 5: e202201470. <https://doi.org/10.26508/lsa.202201470>
- 430 [44] SHARMA N, SETIAWAN D, HAMELBERG D, NARAYAN R, ANEJA R. Computational  
431 benchmarking of putative KIFC1 inhibitors. *Med Res Rev* 2023; 43: 293-318.  
432 <https://doi.org/10.1002/med.21926>
- 433 [45] RATH O, KOZIELSKI F. Kinesins and cancer. *Nat Rev Cancer* 2012; 12: 527-539.  
434 <https://doi.org/10.1038/nrc3310>
- 435 [46] FAN G, SUN L, MENG L, HU C, WANG X et al. The ATM and ATR kinases regulate  
436 centrosome clustering and tumor recurrence by targeting KIFC1 phosphorylation. *Nat*  
437 *Commun* 2021; 12: 20. <https://doi.org/10.1038/s41467-020-20208-x>
- 438 [47] KWON M, GODINHO SA, CHANDHOK NS, GANEM NJ, AZIOUNE A et al.  
439 Mechanisms to suppress multipolar divisions in cancer cells with extra centrosomes. *Genes*  
440 *Dev* 2008; 22: 2189-2203. <https://doi.org/10.1101/gad.1700908>
- 441 [48] LIU J, LI J, TUO Z, HU W, LIU J. BATF2 inhibits PD-L1 expression and regulates CD8+  
442 T-cell infiltration in non-small cell lung cancer. *J Biol Chem* 2023; 299: 105302.  
443 <https://doi.org/10.1016/j.jbc.2023.105302>
- 444 [49] WEN H, TANG J, CUI Y, HOU M, ZHOU J. m6A modification-mediated BATF2  
445 suppresses metastasis and angiogenesis of tongue squamous cell carcinoma through  
446 inhibiting VEGFA. *Cell Cycle* 2023; 22: 100-116.  
447 <https://doi.org/10.1080/15384101.2022.2109897>
- 448 [50] LIU Z, WEI P, YANG Y, CUI W, CAO B et al. BATF2 Deficiency Promotes Progression in  
449 Human Colorectal Cancer via Activation of HGF/MET Signaling: A Potential Rationale for  
450 Combining MET Inhibitors with IFNs. *Clin Cancer Res* 2015; 21: 1752-1763.  
451 <https://doi.org/10.1158/1078-0432.Ccr-14-1564>
- 452 [51] LI Y, FAN L, YAN A, REN X, ZHAO Y et al. Exosomal miR-361-3p promotes the viability  
453 of breast cancer cells by targeting ETV7 and BATF2 to upregulate the PAI-1/ERK pathway.  
454 *J Transl Med* 2024; 22: 112. <https://doi.org/10.1186/s12967-024-04914-4>

- 455 [52] ZONG Y, CHANG Y, HUANG K, LIU J, ZHAO Y. The role of BATF2 deficiency in  
456 immune microenvironment rearrangement in cervical cancer - New biomarker benefiting  
457 from combination of radiotherapy and immunotherapy. *Int Immunopharmacol* 2024; 126:  
458 111199. <https://doi.org/10.1016/j.intimp.2023.111199>
- 459 [53] CAO L, WENG K, LI L, LIN G, ZHAO Y et al. BATF2 inhibits the stem cell-like properties  
460 and chemoresistance of gastric cancer cells through PTEN/AKT/ $\beta$ -catenin pathway.  
461 *Theranostics* 2024; 14: 7007-7022. <https://doi.org/10.7150/thno.98389>
- 462 [54] WEBER AM, RYAN AJ. ATM and ATR as therapeutic targets in cancer. *Pharmacol Ther*  
463 2015; 149: 124-138. <https://doi.org/10.1016/j.pharmthera.2014.12.001>
- 464 [55] HUANG C, FILIPPONE NR, REINER T, ROBERTS S. Sensors and Inhibitors for the  
465 Detection of Ataxia Telangiectasia Mutated (ATM) Protein Kinase. *Mol Pharm* 2021; 18:  
466 2470-2481. <https://doi.org/10.1021/acs.molpharmaceut.1c00166>
- 467 [56] JIANG Q, CHEN Z, MENG F, ZHANG H, CHEN H et al. CD36-BATF2/MYB Axis  
468 Predicts Anti-PD-1 Immunotherapy Response in Gastric Cancer. *Int J Biol Sci* 2023; 19:  
469 4476-4492. <https://doi.org/10.7150/ijbs.87635>
- 470 [57] LI BY, LI HL, ZENG FE, LUAN XY, LIU BQ et al. Identification of PD-L1-related  
471 biomarkers for selecting gastric adenocarcinoma patients for PD-1/PD-L1 inhibitor therapy.  
472 *Discov Oncol* 2025; 16: 689. <https://doi.org/10.1007/s12672-025-02515-1>

473

#### 474 **Figure Legends**

475

476 **Figure 1.** BATF2 mediates chemosensitivity of NCI-N87 cells to ADR and VCR. A) protein  
477 expression of BATF2 in different cells determined by Western blot; B) mRNA expression of BATF2  
478 after overexpression or inhibition in two drug-resistant cells; C) CCK-8 assay for determining the  
479 cell viability after BATF2 overexpression or inhibition; D) representative images of flow cytometry  
480 for analyzing cell apoptosis after BATF2 overexpression or inhibition; E) Quantification of cells  
481 apoptosis determined by flow cytometry. \* $p < 0.05$ , \*\* $p < 0.01$

482

483 **Figure 2.** BATF2 regulates KIFC1 expression and centrosome clustering. A) protein bands (upper)  
484 and quantification (lower) of KIFC1 in two drug-resistant cells after BATF2 overexpression or  
485 inhibition; B) representative immunofluorescence images (left) and corresponding quantification  
486 (right) of the proportion of cells with centrosome cluster after BATF2 overexpression or inhibition.  
487 \* $p < 0.05$ , \*\* $p < 0.01$

488

489 **Figure 3.** BATF2 mediates ATM phosphorylation in drug-resistant cells. A) level of p-ATM/ATM in  
490 NCI-N87 cells and drug-resistant NCI-N87 cells determined by Western blot; B) Western blot bands

491 of Co-IP for investigating the interactions between BATF2 and ATM; C) levels of p-ATM/ATM  
492 after BATF2 overexpression or inhibition. \*p < 0.05, \*\*p < 0.01

493

494 **Figure 4.** BATF2 promotes chemosensitivity by inhibiting ATM phosphorylation. A) protein bands  
495 and quantification of BATF2, ATM and p-ATM expression in each group; B) cell viability of cells  
496 in each treatment group determined by CCK-8 assay; C, representative images (left) and  
497 corresponding quantification (right) of flow cytometry for analyzing cell apoptosis in each  
498 treatment group. \*p < 0.05, \*\*p < 0.01

499

500 **Figure 5.** BATF2 restrains centrosome clustering by inhibiting ATM phosphorylation. A) protein  
501 bands (upper) and quantification (lower) of KIFC1 expression in two drug-resistant cells in each  
502 group; B) representative immunofluorescence images (left) and corresponding quantification (right)  
503 of the proportion of cells with centrosome cluster in each group. \*p < 0.05, \*\*p < 0.01

504

505 **Figure 6.** ATM inhibitor reverses the effects of BATF2 knockdown on cells viability and apoptosis.  
506 A) protein bands and quantification of ATM and p-ATM expression in each group; B) cell viability  
507 of cells in each treatment group determined by CCK-8 assay; C) representative images (left) and  
508 corresponding quantification (right) of flow cytometry for analyzing cell apoptosis in each  
509 treatment group. \*p < 0.05, \*\*p < 0.01

510

511 **Figure 7.** Overview of the mechanism under BATF2-mediated MDR in GC.

Fig. 1 [Download full resolution image](#)

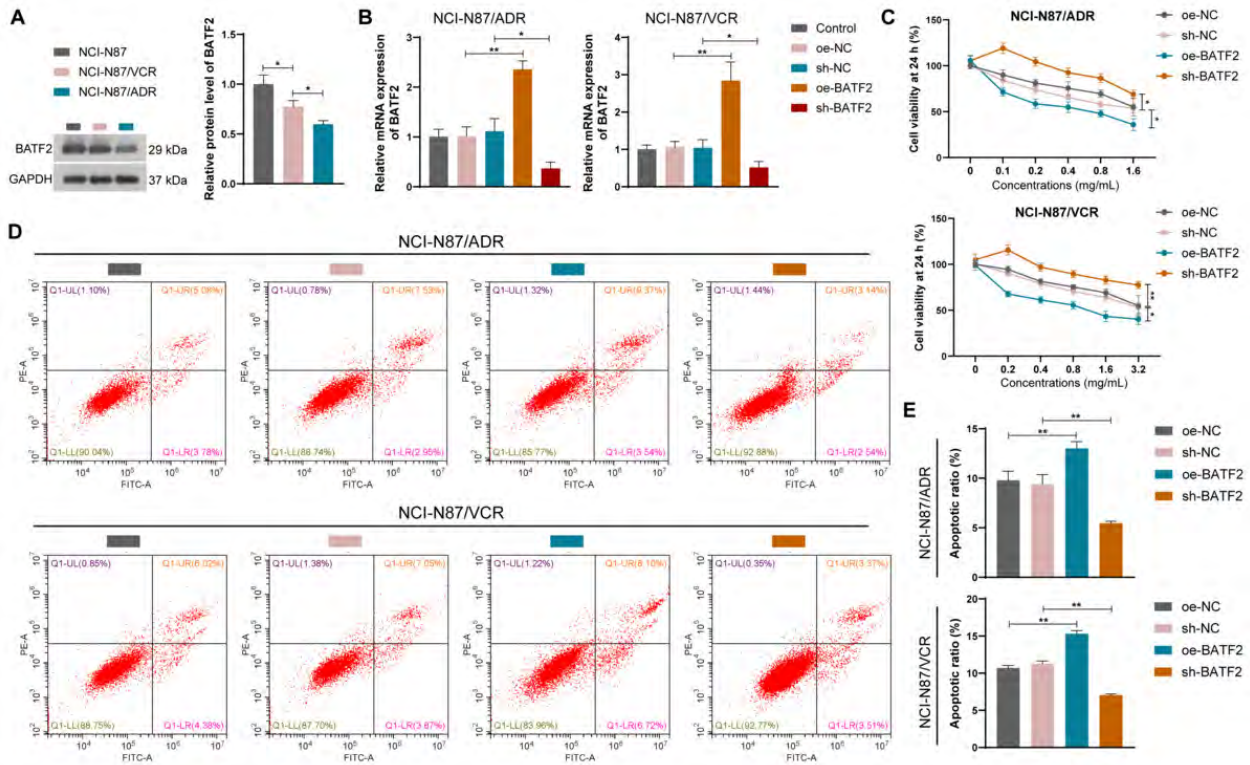


Fig. 2 [Download full resolution image](#)

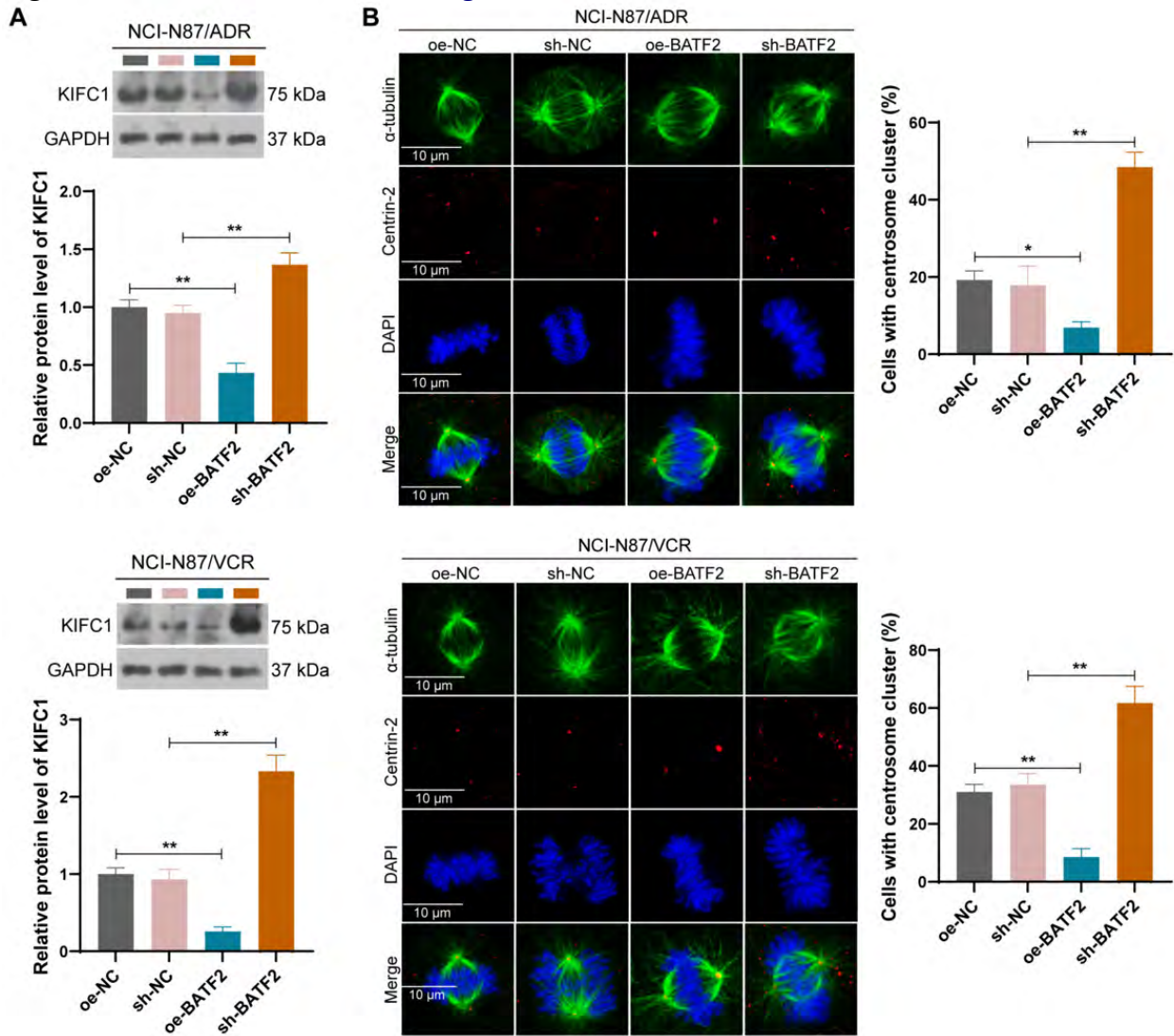


Fig. 3 [Download full resolution image](#)

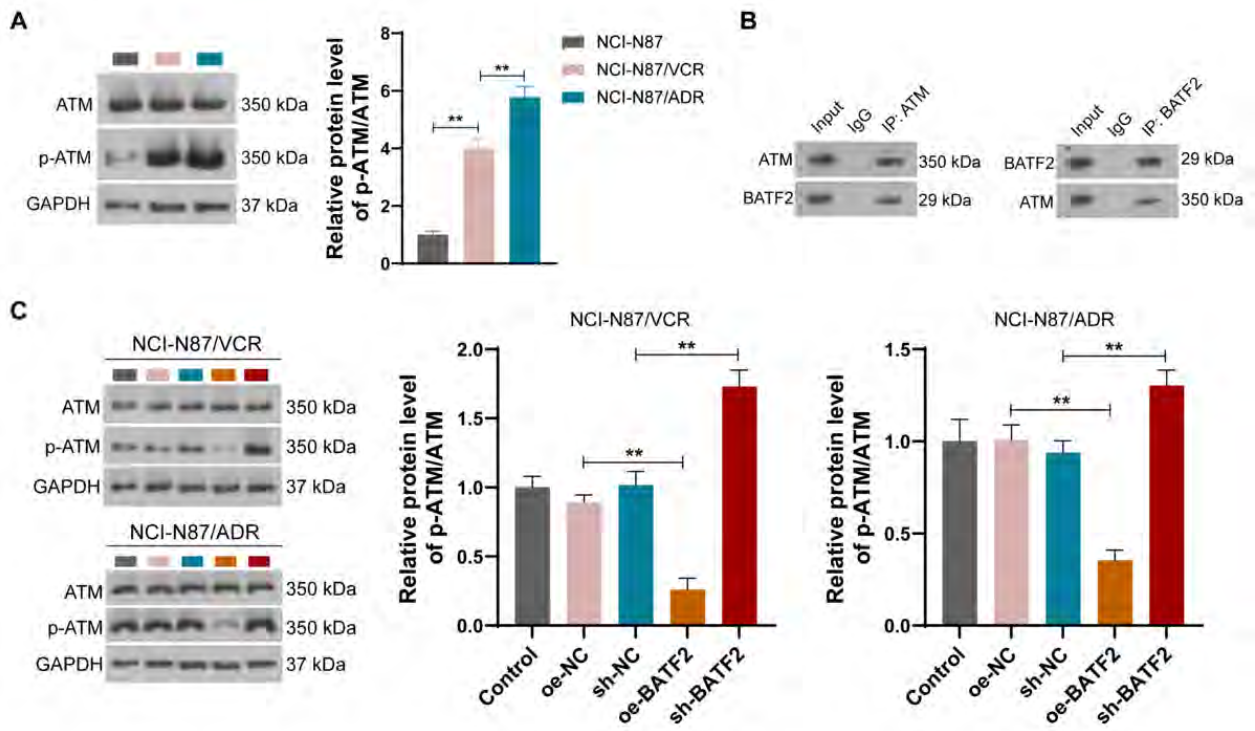


Fig. 4 [Download full resolution image](#)

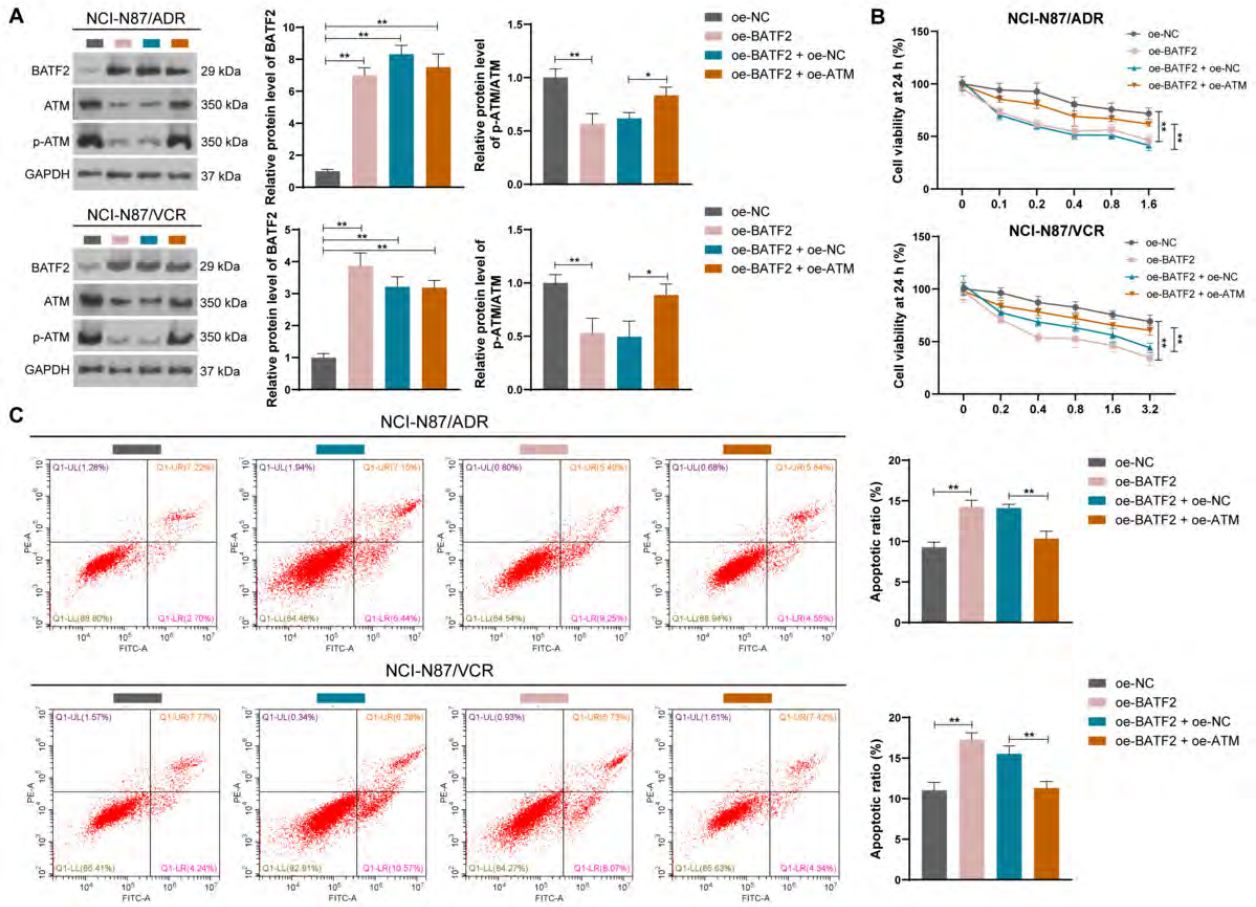


Fig. 5 [Download full resolution image](#)

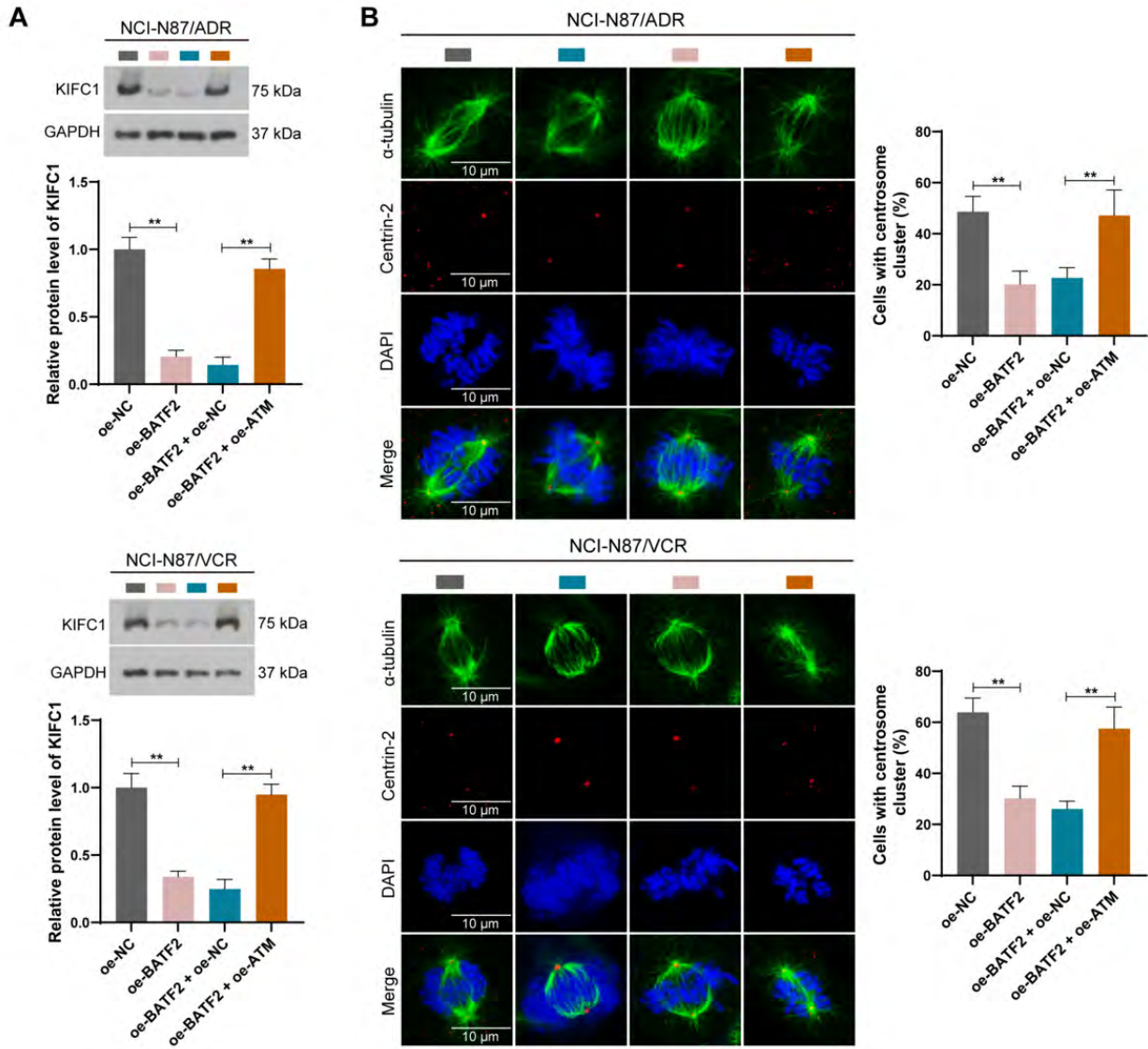


Fig. 6 [Download full resolution image](#)

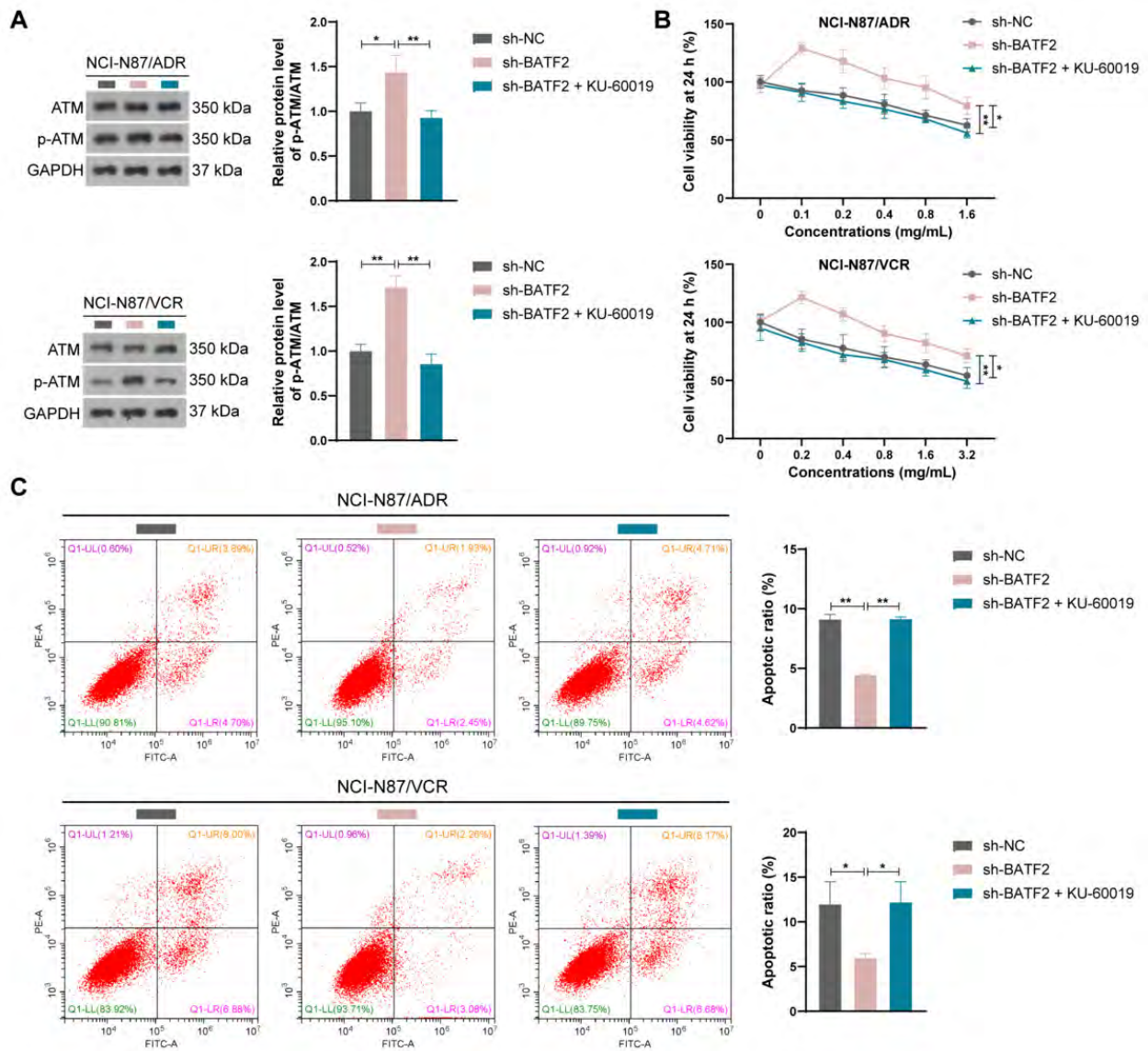


Fig. 7 [Download full resolution image](#)

